Monte Carlo simulation of the motions associated with a single Rouse segment

Y.-H. Lin and Z.-H. Luo

Citation: The Journal of Chemical Physics **112**, 7219 (2000); doi: 10.1063/1.481286
View online: http://dx.doi.org/10.1063/1.481286
View Table of Contents: http://scitation.aip.org/content/aip/journal/jcp/112/16?ver=pdfcov
Published by the AIP Publishing

Monte Carlo simulation of the motions associated with a single Rouse segment

Y.-H. Lin[a] and Z.-H. Luo
Department of Applied Chemistry, National Chiao Tung University, Hsinchu, Taiwan, Republic of China

(Received 27 July 1999; accepted 1 February 2000)

The validity of the Monte Carlo simulation for studying the dynamics of a Rouse chain with a finite number of beads, N, is established by showing the close agreement between the simulation results and the analytical solutions for the time-correlation function of the end-to-end vector. Then, the Monte Carlo simulation is used to calculate the dynamic functions associated with the bond vector $\mathbf{b}(t)$ or direction $\mathbf{u}(t)=\mathbf{b}(t)/|\mathbf{b}(t)|$ of an elastic dumbbell and a Rouse segment in a chain. The effect of chain connectivity on the motions of a single Rouse segment is studied. In particular, it is shown that the dynamic function $\langle P_2[\mathbf{u}(0)\cdot\mathbf{u}(t)]\rangle^2$ over a wide dynamic range, which is the main region probed by the depolarized photon-correlation spectroscopy, is basically independent of the values of $N\geqslant 8$ in agreement with the experimental results. Furthermore, the line shape of the depolarized photon-correlation functions of the concentrated solutions ($\approx$60 wt. %) of polystyrene in cyclohexane at the theta point can be fully accounted for by including the effect of chain connectivity regardless of the crudeness of the Rouse segment relative to the chemical structure. From this study, the molecular weight for a Rouse segment of polystyrene in the concentrated solutions is estimated to be 1100, which is slightly larger than the values $m=780-900$ obtained for polystyrene in the melt state by other methods.
[S0021-9606(00)50316-X]

INTRODUCTION

Slow polymer dynamic and viscoelastic behavior in an entanglement-free system can be well described by theories developed in terms of the Rouse segment as the basic structural unit.[1–3] If our interest is not limited to the slow modes of motions of a long polymer chain, we have to ask how short the Rouse segment can be as it is defined statistically. Related to this is the early studies of the Kuhn segment (considered as equivalent to the Rouse segment) based on the determination of the persistence length by neutron scattering.[4,5] In the recent years, there was much research interest in the subject; and different approaches had been taken: (1) The Rouse segment size was calculated from the high frequency rubbery modulus determined by analyzing the measured dynamic viscoelastic and birefringence spectra with the assumption of a modified stress-optical rule for glassy polymer.[6,7] (2) Through a theoretical analysis relating the depolarized photon-correlation and viscoelastic results of a polystyrene melt, the dynamics and size of a ''Rouse'' segment can be studied.[8–10] (3) The line shapes of the viscoelastic spectra of a series of the polystyrene blends in the entanglement-free region have been analyzed in terms of the Rouse model for the high-molecular-weight component and the elastic dumbbell model for the low-molecular-weight component. The best value for the Rouse segment size occurs, when the viscoelastic spectrum is best described by the theory in both the low and high frequency regions corresponding to the viscoelastic responses of the high- and small-molecular weight components, respectively.[11] The values for the molecular weight of a Rouse segment of polystyrene obtained by these studies range from 780 to 900.

In the second approach listed above, it has been shown that the collective motion observed by the depolarized Rayleigh is basically that associated with a Rouse segment. If each Rouse segment is treated as an elastic dumbbell and undergoes the freely rotational diffusion motion, the correlation time τ_r for $\langle P_2[\mathbf{u}(0)\cdot\mathbf{u}(t)]\rangle$ [where $\mathbf{u}(t)$ is the unit vector indicating the orientation of the Rouse segment; and P_2 is the second-order Legendre polynomial], which is the dynamic function probed by the depolarized photon-correlation spectroscopy, can be obtained to be

$$\tau_r=\zeta'\langle b^2\rangle/18kT=\zeta\langle b^2\rangle/36kT, \tag{1}$$

where ζ' is the friction constant experienced by each bead on the elastic dumbbell, which is half the friction constant ζ for each bead on the Rouse chain ($\zeta/\zeta'=2$, because the mass of an elastic dumbbell is treated as equivalent to that of a Rouse segment; and the mass of the bead of the former is half that of the latter). On the other hand, the relaxation time of the highest Rouse viscoelastic mode is given by

$$\tau_v=\zeta\langle b^2\rangle/24kT=K\pi^2m^2/24 \tag{2}$$

with the friction factor K given by

$$K=\zeta\langle b^2\rangle/kT\pi^2m^2, \tag{3}$$

where m is the molecular weight of a Rouse segment.[12,13] With the m value known, τ_v can be calculated from the viscoelastic data, such as the zero shear viscosity, which is given by

$$\eta_0=(cRT\pi^2/36)KM, \tag{4}$$

where c is the weight amount of polymer per unit volume; and M the molecular weight of the polymer sample.

[a]Author to whom correspondence should be addressed.

Equations (1) and (2) indicates that the two characteristic time constants as can be obtained by the depolarized photon-correlation and viscoelasticity measurements have the same temperature dependence (that of ζ, which is often described by the WLF equation[14]) and the same order of magnitude. These expectations have been supported by the results of the depolarized photon-correlation and viscoelasticity measurements.

In obtaining Eq. (1), the connections of each Rouse segment in both ends to the rest of the chain are neglected. The connection of the Rouse segments in a chain gives rise to the Rouse normal modes of motions. Based on the Rouse model, the viscoelastic spectrum and the time correlation function of the end-to-end vector can be theoretically expressed in terms of the normal modes.[1–3] The dynamic functions, $\langle \mathbf{u}_s(0)\cdot\mathbf{u}_s(t)\rangle$ and $\langle P_2[\mathbf{u}_s(0)\cdot\mathbf{u}_s(t)]\rangle$ associated with a single Rouse segment, which do not have an analytical solution, can be calculated by the Monte Carlo simulation based on the Langevin equation.

With the effect of the connection between neighboring Rouse segments included, any dynamic function associated with a single Rouse segment is expected to be nonsingle-exponential. It is well known that the depolarized photon-correlation function of a polymer melt or concentrated solution is not a single exponential.[15,16] This study allows us to study the chain connectivity in affecting the non-single-exponential decaying behavior.

First, we shall establish the validity of the Monte Carlo simulation by the comparison with the analytical solution for the time-correlation function of the end-to-end vector $\langle \mathbf{R}(0)\cdot\mathbf{R}(t)\rangle$ of a Rouse chain with a finite number of beads, N. Then we can use the Monte Carlo simulation to calculate the time correlation functions,

$$C_{0s}(t)=\langle \mathbf{b}_s(0)\cdot\mathbf{b}_s(t)\rangle/\langle b_s^2\rangle, \tag{5}$$

$$C_{1s}(t)=\langle \mathbf{u}_s(0)\cdot\mathbf{u}_s(t)\rangle \tag{6}$$

and

$$C_{2s}(t)=\langle P_2[\mathbf{u}_s(0).\mathbf{u}_s(t)\rangle], \tag{7}$$

where $\mathbf{b}_s(t)$ is the bond vector of the sth Rouse segment at time t and $\mathbf{u}_s(t)=\mathbf{b}_s(t)/|\mathbf{b}_s(t)|$. Before the effect of chain connectivity as reflected by the above dynamic functions is studied, we shall examine by the Monte Carlo simulation how well in the elastic dumbbell case $C_0(t)=\langle \mathbf{b}(0)\cdot\mathbf{b}(t)\rangle/\langle b^2\rangle$ can be approximated by $C_1(t)=\langle \mathbf{u}(0)\cdot\mathbf{u}(t)\rangle$ [where $\mathbf{u}(t)=\mathbf{b}(t)/|\mathbf{b}(t)|$] and how applicable is the freely rotational diffusion model in relating $C_0(t)$ [or $C_1(t)$] and $C_2(t)=\langle P_2[\mathbf{u}(0)\cdot\mathbf{u}(t)]\rangle$. And finally the average $\Sigma_{s=1,N-1}C_{2s}(t)/(N-1)$ in a Rouse chain will be studied as a function of N and compared with the results of the depolarized photon-correlation measurements.

THE LANGEVIN EQUATION

Consider a linear Gaussian chain with N beads, whose configuration is represented by the set of N position vectors of the beads $\{\mathbf{R}_n\}\equiv(\mathbf{R}_1,\mathbf{R}_2,\mathbf{R}_3,\ldots,\mathbf{R}_N)$. While the movement of each bead is hindered by a friction force characterized by the friction constant ζ, it receives the random force $\mathbf{f}_n(t)=(\zeta\mathbf{g}_n(t))$ due to the incessant collisions of the bead (the Brownian particle) with the fluid molecules or segments. Then the motions of the chain are described by the Langevin equations[2,9]

$$d\mathbf{R}_n/dt=-(3kT/\langle b^2\rangle\zeta)(2\mathbf{R}_n-\mathbf{R}_{n+1}-\mathbf{R}_{n-1})+\mathbf{g}_n(t) \tag{8}$$

for the internal beads $(n=2,3,4,\ldots,N-1)$ and

$$d\mathbf{R}_1/dt=-(3kT/\langle b^2\rangle\zeta)(\mathbf{R}_1-\mathbf{R}_2)+\mathbf{g}_1(t), \tag{9}$$

$$d\mathbf{R}_N/dt=-(3kT/\langle b^2\rangle\zeta)(\mathbf{R}_N-\mathbf{R}_{N-1})+\mathbf{g}_N(t), \tag{10}$$

for the end beads ($n=1$ and N). The random fluctuation $\mathbf{g}_n$ is Gaussian and characterized by the moments

$$\langle \mathbf{g}_n(t)\rangle=0, \tag{11}$$

$$\langle g_{n\alpha}(t)g_{m\beta}(t')\rangle=2D\delta_{nm}\delta_{\alpha\beta}\delta(t-t'), \tag{12}$$

where $D(=kT/\zeta)$ is the diffusion constant of a free bead; and α, β represent the x, y, z coordinates.

The bond vectors $\{\mathbf{b}_s\}$ and the end-to-end vector $\mathbf{R}$ are defined, respectively, as

$$\mathbf{b}_s=\mathbf{R}_{s+1}-\mathbf{R}_s, \tag{13}$$

$$\mathbf{R}=\mathbf{R}_N-\mathbf{R}_1=\Sigma_{s=1,N-1}\mathbf{b}_s. \tag{14}$$

Following the usual procedure of transformation to the normal coordinates,[1,17] the time correlation function of the end-to-end vector $\mathbf{R}(t)$ is obtained as

$$\langle \mathbf{R}(0)\cdot\mathbf{R}(t)\rangle=\Sigma_{p=\text{odd},1\text{ to }N-1}(2\langle b^2\rangle/N)\times[\cos^2(p\pi/2N)/\sin^2(p\pi/2N)]\times\exp(-t/\tau_p) \tag{15}$$

with $\Sigma_{p=\text{odd},1\text{ to }N-1}$ meaning summation over odd p's from 1 to $N-1$, and

$$\tau_p=\zeta\langle b^2\rangle/[12kT\sin^2(p\pi/2N)]=K\pi^2M^2/[12N^2\sin^2(p\pi/2N)], \tag{16}$$

where K is given by Eq. (3).

When $N\to\infty$, Eq. (15) in combination with Eq. (16) reduces to the result obtained from the continuous Rouse chain model.[2]

The time correlation function of $\mathbf{b}_s(t)$ [Eq. (5)] is obtained in terms of the normal modes as

$$C_{0s}(t)=(2/N)\Sigma_{p=1,N-1}\sin^2(sp\pi/N)\exp(-t/\tau_p). \tag{17}$$

THE MONTE CARLO SIMULATION

In the Monte Carlo simulation, the Langevin equation is replaced by the calculation of the positions of the beads at the next step $\{\mathbf{R}_n(t_i+\Delta t)\}$ from their positions $\{\mathbf{R}_n(t_i)\}$ at some present time t_i (note $t_{i+1}=t_i+\Delta t$).[18,19] Corresponding to Eq. (8),

$$\mathbf{R}(t_i+\Delta t)=\mathbf{R}(t_i)-S[2\mathbf{R}_n(t_i)-\mathbf{R}_{n+1}(t_i)-\mathbf{R}_{n-1}(t_i)]+\mathbf{d}_{ni}, \tag{18}$$

where

$$S=3D\Delta t/\langle b^2\rangle, \tag{19}$$

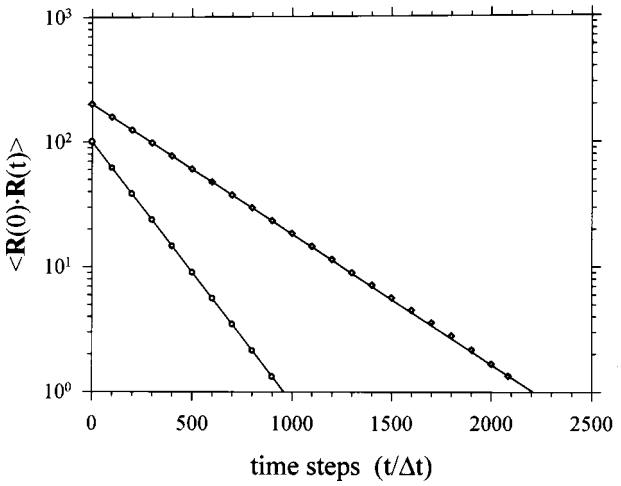

FIG. 1. Comparison of the analytical solution (the solid line) and the Monte Carlo simulation for the time correlation function of the end-to-end vector $\mathbf{R}(t)$ of the Rouse chain with $N=2$ (○) and with $N=3$ (◇).

and the random displacement $\mathbf{d}_{ni}$ is Gaussian and characterized by the moments,

$$\langle \mathbf{d}_{ni} \rangle = 0, \tag{20}$$

$$\langle d_{\alpha ni} d_{\beta mj} \rangle = \delta_{\alpha,\beta} \delta_{n,m} \delta_{i,j} 2D\Delta t, \tag{21}$$

where α, β represent the x,y,z coordinates (for instance d_x represent the x-component of $\mathbf{d}$). Equations equivalent to Eq. (18) can similarly be written for Eqs. (9) and (10). Dependent on the choice of $2D\Delta t = l^2$ in the Monte Carlo simulation, the number of time steps corresponding to τ_p [Eq. (16)] is given by

$$\tau_p / \Delta t = (\langle b^2 \rangle / l^2)/6 \sin^2(p\pi/2N). \tag{22}$$

COMPARISON OF THE SIMULATION RESULTS AND THE ANALYTICAL SOLUTIONS

We have chosen the simple chain systems, $N=2$, 3, and 5 for making the comparison between simulation and theory. According to Eq. (15), only a single relaxation mode occurs in the time correlation function of the end-to-end vector in either the $N=2$ or the $N=3$ system; and two relaxation modes in the case of $N=5$. Shown in Fig. 1 are the comparisons of the simulation results of $N=2$ and $N=3$ with Eq. (15) in combination with Eq. (22). The chosen parameters in the simulation are $\langle b^2 \rangle^{0.5} = 10$, and $l=0.4$. The shown simulation results are the outcomes of averaging over 4×10^8 steps. As shown in Fig. 1 for $N=2$ and 3, both the initial values and the relaxation times obtained from the simulation are in close agreement with the theoretical results. In the case of $N=5$, similar close agreement between theory and simulation is obtained. The results shown in Figs. 1 as well as that obtained for $N=5$ illustrate that the chain dynamics as described by the Langevin equations [Eqs. (8)–(12)] can be faithfully calculated by the Monte Carlo simulation. Thus, the Monte Carlo simulation can be used to calculate dynamic functions of a physical quantity or of a system with additional effects, which are impossible to obtain analytically.

THE MOTION OF AN ELASTIC DUMBBELL

The elastic dumbbell model is a special case of the Rouse chain model. The dynamic behavior $C_0(t) = \langle \mathbf{b}(0) \cdot \mathbf{b}(t) \rangle / \langle b^2 \rangle$ [Eq. (5)] for the elastic dumbbell can be obtained from the Langevin equations to be a single exponential decay as shown in Fig. 1. $C_0(t)$ being a single exponential decay suggests that the elastic dumbbell motion may be sufficiently well described by the free rotational diffusion model. Based on the freely rotational diffusion model,[20] the dynamic function $C_2(t) = \langle P_2[\mathbf{u}(0) \cdot \mathbf{u}(t)] \rangle$ [Eq. (7)] is expected to be a single exponential decay with the relaxation time being one third of that of $C_0(t)$ [see Eq. (1)]. How well the free rotational diffusion model describe $C_2(t)$ of an elastic dumbbell can be studied by the Monte Carlo simulation. However, in the simulation calculation of $C_2(t)$, we need to assume $\mathbf{u}(t) = \mathbf{b}(t)/|\mathbf{b}(t)|$. From comparing Eqs. (5) and (7), this means that we have assumed that $\mathbf{b}(t)/\langle b^2 \rangle^{0.5}$ can be approximated by $\mathbf{u}(t) = \mathbf{b}(t)/|\mathbf{b}(t)|$. We can test this approximation by showing that $C_0(t)$ can be well approximated by $C_1(t) = \langle \mathbf{u}(0) \cdot \mathbf{u}(t) \rangle$ [Eq. (6)].

The relation between $C_1(t)$ and $C_0(t)$ can be analyzed as in the following. Denoting $|\mathbf{b}(t)|$ as $b(t)$ and $\langle |\mathbf{b}| \rangle$ as b_0, we may express $b(t)$ as

$$b(t) = b_0 + \Delta b(t), \tag{23}$$

where $\Delta b(t)$ is the bond length fluctuation. For $\langle b^2 \rangle = 100$ as assumed in this study, we have obtained $b_0 = 9.2$, which is not much smaller than $\langle b^2 \rangle^{0.5}$. This indicates that the fluctuation $\Delta b(t)$ is rather small. This is the main basis for our approximating $C_0(t)$ by $C_1(t)$ and treating the Rouse segment basically as equivalent to a Kuhn segment (for instance, when we relate the viscoelastic data to the depolarized photon correlation results). Using Eq. (23), $C_1(t)$ can be approximately expressed as

$$\begin{aligned} C_1(t) &\approx \langle \mathbf{b}(0) \cdot \mathbf{b}(t) \rangle \langle 1/[b(0)b(t)] \rangle \\ &= \langle \mathbf{b}(0) \cdot \mathbf{b}(t) \rangle \langle 1/[(b_0 + \Delta b(0))(b_0 + \Delta b(t))] \rangle \\ &= \langle \mathbf{b}(0) \cdot \mathbf{b}(t) \rangle \langle 1/[b_0^2 (1 + \Delta b(0)/b_0) \\ &\quad \times (1 + \Delta b(t)/b_0)] \rangle \\ &\approx \langle \mathbf{b}(0) \cdot \mathbf{b}(t) \rangle \langle (1 - \Delta b(0)/b_0) \\ &\quad \times (1 - \Delta b(t)/b_0) \rangle / \langle b^2 \rangle \\ &= C_0(t)[1 + \langle \Delta b(0) \Delta b(t) \rangle / b_0^2]. \end{aligned} \tag{24}$$

Equation (24) mainly shows the dynamic relation between $C_1(t)$ and $C_0(t)$. Both $C_1(t)$ and $C_0(t)$ as they are defined are normalized functions. Because of the approximation steps taken, $C_1(t)$ as expressed by Eq. (24) is not normalized; and need be renormalized. As shown in Fig. 2, after a small initial drop due to the decay of $\langle \Delta b(0) \Delta b(t) \rangle / b_0^2$, the relaxation curves of $C_1(t)$ and $C_0(t)$ parallel each other and maintain a ratio $C_1(t)/C_0(t) = 0.85$. It is also shown in Fig. 2 that the agreement between $C_1(t)$ obtained directly from the simulation and $C_1(t)$ calculated from Eq. (24) using the simulation results of $C_0(t)$ and $\langle \Delta b(0) \Delta b(t) \rangle$ and renormalized is very good.

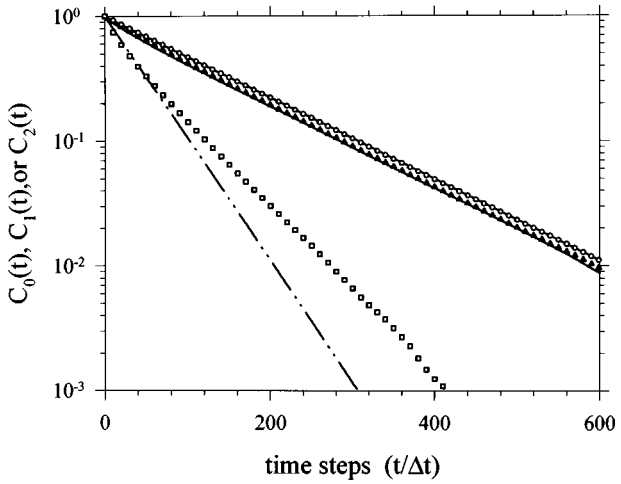

FIG. 2. Comparison of the analytic solution (the upper solid line) and the simulation (○) for $C_0(t)$; comparison of $C_1(t)$ obtained directly from simulation (△) and calculated from Eq. (24) using the simulation results of $C_0(t)$ and $\langle \Delta b(0)\Delta b(t)\rangle$ (the lower solid line); Comparison of $C_2(t)$ obtained from simulation (□) and expected based on $C_0(t)$ and the freely rotational diffusion model (· · –). All the shown dynamic functions are for the elastic dumbbell.

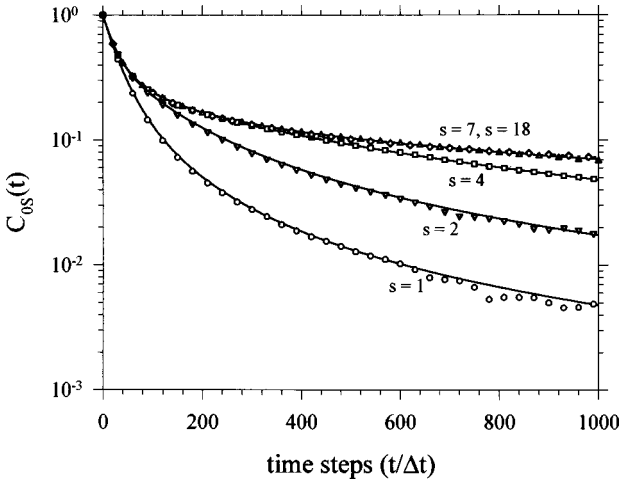

FIG. 3. Comparison of the simulation results of $C_{0s}(t)$ (○ for $s=1$; ▽ for $s=2$; □ for $s=4$; △ for $s=7$; and ◇ for $s=18$) and those calculated from Eq. (17) for the Rouse chain with $N=36$ (the solid lines from left to right are for $s=1$, 2, 4, and 7 respectively; while the dotted line is for $s=18$, which is virtually superposed on the line for $s=7$). The simulation results are symmetrical with respect to the center of the chain; and the results of only one side are shown.

Also shown in Fig. 2 is the comparison of the theoretical curve of $C_2(t)$ based on using the free rotational diffusion model in relating $C_0(t)$ and $C_2(t)$, and the simulation curve of $C_2(t)$. One can notice that in the short time region (down to $C_2(t)=0.3\approx e^{-1}$), the simulation result of $C_2(t)$ can be well described by the free rotational diffusion model, while, the whole simulated $C_2(t)$ curve is not a single exponential decay. Overall, the elastic dumbbell dynamic behavior is not far from described by the free rotational diffusion model as revealed in terms of the comparison of $C_0(t)$ [or $C_1(t)$] and $C_2(t)$. The simulation result of $C_2(t)$ in particular will serve as a reference for comparison with the dynamic behavior of a Rouse segment in a chain to study the effect of chain connectivity.

THE MOTION OF A ROUSE SEGMENT IN A CHAIN

As expected intuitively, the simulated $C_{0s}(t)$, $C_{1s}(t)$, and $C_{2s}(t)$ dynamic processes become slower gradually, as the monitored segment (denoted by the index s) is shifted from the chain end to the middle of the chain as shown in Figs. 3, 4, and 5 (to avoid congestion in the figures, only results at a few selected s values are shown). The shown results for a chain with $N=36$ indicate that the dynamic functions over the whole range become basically independent of s for $s=7-18$. In other words, the dynamic functions of a segment, which is only a few segments away from the chain end is free of the chain end effect and become independent of s. In particular, $C_{2s}(t)$ over a wide of dynamic range (≈one and a half orders) is very much independent of s for $s\geqslant 2$. It is shown in Fig. 3 that the simulation results of $C_{0s}(t)$ at different s values are in close agreement with the curves calculated from Eq. (17). As expected, the dynamic functions obtained from the simulation are symmetric with respect to the center of the chain i.e., the dynamic function at the sth segment is the same as that at the $(N\text{-}s)$th segment. Experimentally (for example, in the depolarized photon-correlation spectroscopy), it is often the average of the dynamic functions, that are probed. Thus, we define

$$\langle C_0(t)\rangle = (\Sigma_{s=1,N-1} C_{0s}(t))/(N-1), \tag{25}$$

$$\langle C_1(t)\rangle = (\Sigma_{s=1,N-1} C_{1s}(t))/(N-1), \tag{26}$$

and

$$\langle C_2(t)\rangle = (\Sigma_{s=1,N-1} C_{2s}(t))/(N-1). \tag{27}$$

Shown in Fig. 6 is the comparison of $\langle C_0(t)\rangle$, $\langle C_1(t)\rangle$, and $\langle C_2(t)\rangle$ for a chain with $N=36$. While $\langle C_0(t)\rangle$ is no longer a single exponential decay as $C_0(t)$, the relative differences among $\langle C_0(t)\rangle$, $\langle C_1(t)\rangle$, and $\langle C_2(t)\rangle$ are similar to those among $C_0(t)$, $C_1(t)$, and $C_2(t)$ as shown in Fig. 2 for the elastic dumbbell case.

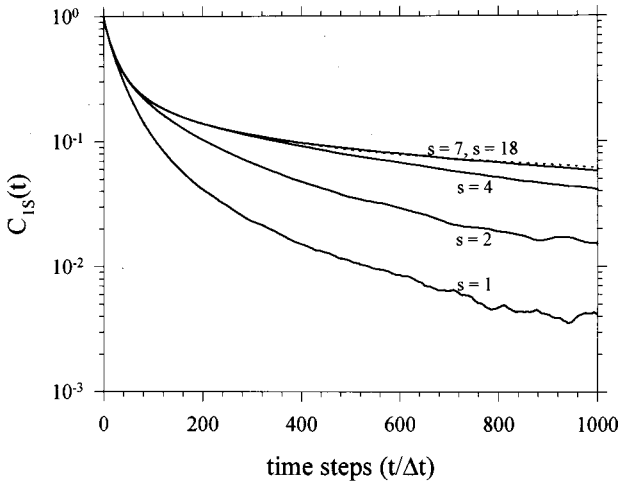

FIG. 4. The simulation results of $C_{1s}(t)$ as a function of s (the solid lines from left to right are for $s=1$, 2, 4, and 7, respectively, while the dotted line is for $s=18$).

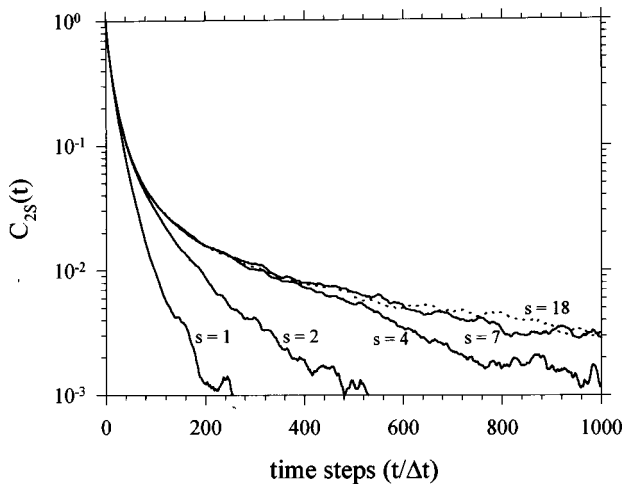

FIG. 5. The simulation results of $C_{2s}(t)$ as a function of s (see Fig. 4).

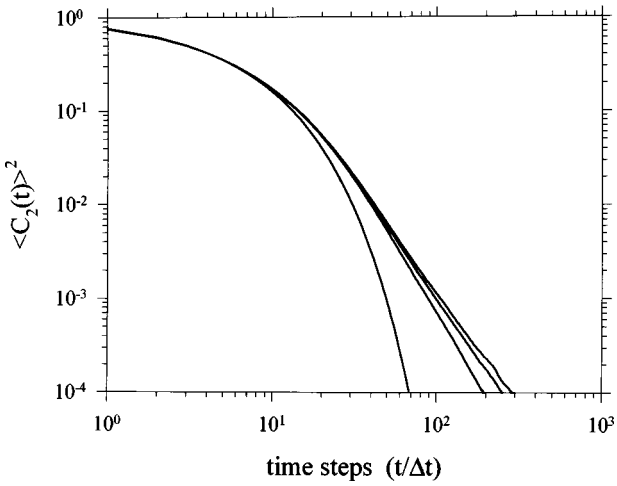

FIG. 7. Comparison of the simulation results of $\langle C_2(t)\rangle^2$ of the Rouse chains with $N=2$ (the first line from the left), 8 (the second from the left), 16 (the third from the left), and 36 (the first from the right).

What is particularly interesting to us is the $\langle C_2(t)\rangle$ dynamic process for comparison with the depolarized photon-correlation results. The dynamic function directly observed from the photon-correlation spectroscopy is the square of $\langle C_2(t)\rangle$. In Fig. 7, we show the comparison of the $\langle C_2(t)\rangle^2$ curves calculated for $N=2$, 8, 16, and 36. It can be seen that the relaxation time distributions for $N=8$, 16, and 36 is significantly broader than that of the elastic dumbbell case ($N=2$) and that in the short time region (down to $\langle C_2(t)\rangle^2=0.01$), basically there is no difference among the curves for different values of $N\geqslant 8$. Mainly the tail region of the relaxation curve is slowly moved to the longer time with increasing N. In other words, the short time region of $\langle C_2(t)\rangle^2$ is mainly affected by the local motion, which is independent of the molecular weight, the tail region of the relaxation curve is weakly affected by the slow modes of the Rouse chain, which is molecular weight dependent. As $C_{2s}(t)$ is least dependent on s over a large dynamic range as pointed out above, $\langle C_2(t)\rangle$ is much less affected by the molecular weight change than $\langle C_0(t)\rangle$ and $\langle C_1(t)\rangle$.

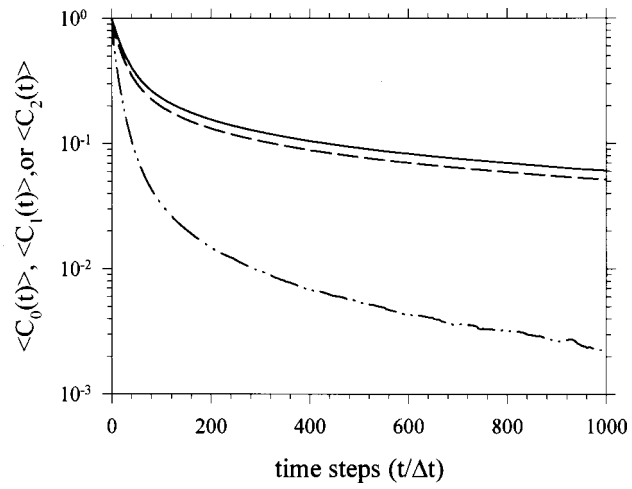

FIG. 6. Comparison of the simulation results $\langle C_0(t)\rangle$ (—), $\langle C_1(t)\rangle$ (---), and $\langle C_2(t)\rangle$ (· · –) of the Rouse chain with $N=36$.

In the depolarized photon-correlation spectroscopy, it is mainly the short time region of $\langle C_2(t)\rangle^2$ that is probed.[9,10] The above result is in agreement with the basic molecular weight independence of the depolarized photon-correlation function, that has been observed.

COMPARISON OF SIMULATION AND EXPERIMENT FOR $\langle C_2(t)\rangle^2$

In a polymer system, the static pair correlation as determined from the depolarized intensity measurement is often expressed in terms of effective optical anisotropy δ^2 per monomer unit to account for the concentration dependence of the measured total intensity. In the case of polystyrene,[21,22] it has been shown that the δ^2 value in the melt is virtually the same as in the dilute solution. This result indicates that in a polystyrene concentrated solution or melt system, the segments belonging to different chains do not interact in such a way as to contribute to the static pair correlation. In addition, the dynamic pair correlation is in general much smaller than the static pair correlation.[23,24] Thus, the dynamic depolarized scattering structure factor of a polystyrene concentrated solution or melt system can be simplified greatly by neglecting the cross terms between segments belonging to different chains. The polymer chain can be modeled as a chain of freely jointed Kuhn segments; and the pair correlation terms are limited to the chemical segments belonging to the same Kuhn segment. Using the fact that the chain size is much smaller than the scattering wavelength; and the assumption that the translational motion of the center of mass of the polymer chain (over a distance comparable to the wavelength) is independent of and much slower than the segmental reorientation, the dynamic depolarized scattering structure factor can be reduced to be proportional to[8–10]

$$C_p(t)=[Sf_s(t)+R]\langle P_2[\mathbf{u}(0)\cdot\mathbf{u}(t)]\rangle, \tag{28}$$

where $\mathbf{u}(t)$ is the unit vector representing the the direction of the symmetry axis of the Kuhn segment (regarded as equivalent to the Rouse segment), $f_s(t)$ is the normalized time-correlation function that reflects the motions associated with local chemical bonds (grossly referred to as the sub-Rouse-segmental motions), and the relaxation strength S depends on the details of the bond angles and steric interactions among the chemical bonds. R is a constant and is related to how anisotropy the Rouse segment (or Kuhn segment) is.

For the polystyrene melt, the $f_s(t)$ and $\langle P_2[\mathbf{u}(0)\cdot\mathbf{u}(t)]\rangle$ dynamic processes can not be resolved from the observed depolarized photon-correlation function.[8,9,15] The close overlap of the two processes in the time scale is attributed to the strong direct interactions among segments. The chain dynamics in the concentrated solutions of two nearly monodisperse polystyrene samples (F1 with $M_w=9100$ and F2 with $M_w=18100$) in cyclohexane [the two solutions are denoted as S-F1 (59.832 wt.%) and S-F2 (60.287 wt.%)] have been studied by means of the viscosity and depolarized photon-correlation measurements[10] (see the Appendix). Both the studied systems are in the entanglement-free region; the obtained molecular weight dependence of the zero shear viscosity (adjusted to the same concentration, see the details in Ref. 10) indicates that the chain dynamics are described by the Rouse theory. The applicability of the Rouse theory to the studied systems is in agreement with the expectation that at the high concentrations ($\sim$60 wt.%) the hydrodynamic interaction is much screened.[2,25,26] In these systems, the two processes as contained in Eq. (28) are far apart and can be well resolved. This should be due to the ''lubrication'' effect of the solvent that prevents the strong interactions among segments. The observed slow mode, namely, the $\langle P_2[\mathbf{u}(0)\cdot\mathbf{u}(t)]\rangle$ dynamic process, is independent of the scattering angle and (basically) molecular weight; and has a relaxation time, which has the same order of magnitude as τ_v calculated from the viscosity data [Eq. (2); assuming the molecular weight for a Rouse segment, m, being 1000, which is close to the values 780–900 obtained from other studies].

Since the $f_s(t)$ and $\langle P_2[\mathbf{u}(0)\cdot\mathbf{u}(t)]\rangle$ processes in the S-F1 and S-F2 systems can be well resolved, the contribution of $f_s(t)$ can be removed to obtain the depolarized photon correlation function due to the $\langle P_2[\mathbf{u}(0)\cdot\mathbf{u}(t)]\rangle$ mode for comparison with the simulation results of $\langle C_2(t)\rangle$.

The average relaxation time of $\langle C_2(t)\rangle$ from the simulation can be defined as

$$\langle\tau_r\rangle=\int_0^\infty\langle C_2(t)\rangle dt=\Sigma_{i=1,\infty}\langle C_2(t_i)\rangle\Delta t. \tag{29}$$

Corresponding to the simulation, τ_v can be obtained from Eq. (2) as

$$\tau_v=(\langle b^2\rangle/12l^2)\Delta t. \tag{30}$$

Using Eqs. (29) and (30), from the simulation we obtain $\langle\tau_r\rangle/\tau_v=2.2$, 2.5, and 2.7 for $N=8$, $N=16$, and $N=36$, respectively, which depends on N very weakly.

In Ref. 10, we have obtained the average relaxation time $\langle\tau_r\rangle$ (denoted as $\langle\tau\rangle_2$) for the $\langle P_2[\mathbf{u}(0)\cdot\mathbf{u}(t)]\rangle$ dynamic process from the depolarized photon-correlation function using the MSVD analysis;[27] and $m=1000$ was used to calculate τ_v from Eq. (2) ($\tau_v=\tau_8$ for S-F1 and $\tau_v=\tau_{17}$ for S-F2).

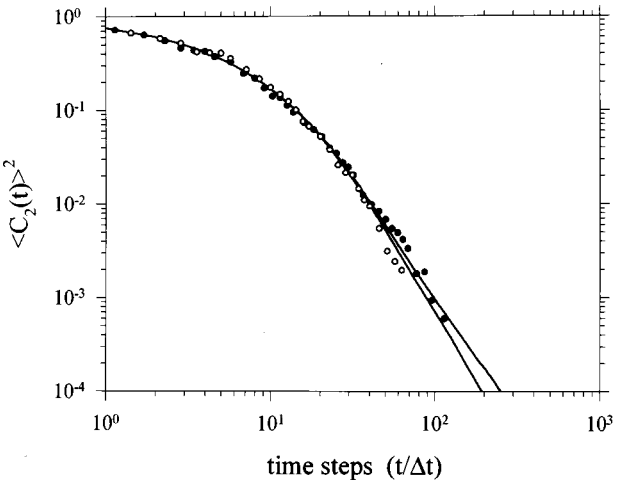

FIG. 8. Comparison of the $\langle P_2[\mathbf{u}(0)\cdot\mathbf{u}(t)]\rangle^2$ dynamic processes obtained from the depolarized photon-correlation functions of the S-F1 (○) and S-F2 (●) samples and the simulation results of $\langle C_2(t)\rangle^2$ of the Rouse chain with $N=8$ (the left solid line) and with $N=16$ (the right solid line).

As listed in Table I of Ref. 10, $\langle\tau_r\rangle/\tau_v=3.0(=\langle\tau\rangle_2/\tau_8)$ for S-F1 and $=3.3$ $(=\langle\tau\rangle_2/\tau_{17})$ (using the results of the 45° scattering angle, at which the photon-correlation functions can be more clearly analyzed by the MSVD method; see Ref. 10 for details). While the $\langle\tau_r\rangle$ value is experimentally determined from the depolarized photon-correlation measurement, the τ_v value calculated from the viscosity data is affected by the choice of the m value. A close agreement of the $\langle\tau_r\rangle/\tau_v$ ratio values with the values obtained from simulation using Eqs. (29) and (30) as listed above can be obtained by choosing the m value to be 1100. Thus, corresponding to $m=1100$, we choose $N=8$ for F1 and $N=16$ for F2. And the simulation results of $\langle C_2(t)\rangle^2$'s for $N=8$ and $N=16$ have been shown in Fig. 7. As shown in Fig. 8, these results are compared with the photon correlation functions, $\langle P_2[\mathbf{u}(0)\cdot\mathbf{u}(t)]\rangle^2$, which have been obtained from the depolarized photon-correlation functions of S-F1 and S-F2 (at the 45° scattering angle) by removing the $f_s(t)$ contribution. Because the vertical magnitude of a depolarized photon correlation function depends on the coherence factor of the instrument, the comparison between simulation and experiment is made by allowing shifting in both the vertical and horizontal (time) coordinates to obtain a good matching of the data points and the simulation results. As shown in Table I of Ref. 10, $\langle\tau_r\rangle$ for S-F1 is about 30% smaller than that for S-F2. This was shown to be due to the small concentration difference and friction constant difference between S-F1 and S-F2 (see Ref. 10 for the details). In matching of the data points and the simulation results as shown in Fig. 8, the $\sim$30% difference between the shifting factors along the time coordinate for the results of S-F1 and S-F2 have been observed. Thus, the close agreement between experiment and simulation as shown in Fig. 8 is consistently obtained for the S-F1 and S-F2 systems.

DISCUSSION AND SUMMARY

A Rouse chain with a finite number of beads, N, is shown to be a good system for investigating some of the

internal dynamic motions of the chain, in particular, the motions associated with the size scale of a Rouse segment by using the Monte Carlo simulation. First, the validity of the Monte Carlo simulation is established by showing the close agreement of the simulation results with the analytical solutions for the time correlation functions of the end-to-end vector. The Monte Carlo simulation can then be used to study the dynamic functions, which do not have an analytical solution. From the simulation, it is shown that $C_0(t)$ can be well approximated by $C_1(t)$ [or $C_{0s}(t)$ by $C_{1s}(t)$ or $\langle C_0(t)\rangle$ by $\langle C_1(t)\rangle$]. This is related to the average Rouse segment length $b_0(=\langle|\mathbf{b}|\rangle)$ being just slightly smaller than $\langle b^2\rangle^{0.5}$.

It is also shown that $\langle P_2[\mathbf{u}(0)\cdot\mathbf{u}(t)]\rangle$ for an elastic dumbbell is not a single exponential, neither is far from described by the freely rotational diffusion model. The relaxation time distribution of the average $\langle P_2[\mathbf{u}(0)\cdot\mathbf{u}(t)]\rangle$ (i.e., $\langle C_2(t)\rangle$) for a Rouse segment in a chain is further broadened by the hindrance effect due to connection to neighboring segments. When the number of the beads in a Rouse chain is sufficiently large ($N\geqslant 8$), the results of $\langle C_2(t)\rangle^2$ for a Rouse segment is basically independent of the molecular weight (N) over a wide dynamic range, which is the main region probed by the depolarized photon-correlation spectroscopy. This is in agreement with the observed molecular weight independence of the $\langle P_2[\mathbf{u}(0)\cdot\mathbf{u}(t)]\rangle$ dynamic process obtained from the depolarized photon-correlation measurement.[10]

The Rouse segment as a structural unit has been mainly useful for describing low frequency motions involving a large section of the polymer chain.[2] Relative to the chemical structure of the polymer chain, the Rouse segment is a rather crude picture. At the size scale between that characteristic of the local chemical structure and the large size scale corresponding to the low frequency modes (i.e., at the Rouse segment size scale), how useful the Rouse segment is for describing the motions has not been much investigated. In the previous analysis of relating the depolarized photon-correlation and viscoelasticity results,[8–10] the use of the Rouse segment allows us to show that the relaxation times $\langle\tau_r\rangle$ and τ_v have the same order of magnitude and the same temperature dependence as supported by the experimental results. The agreement between experiment and simulation shown in Fig. 8 suggests that in a concentrated solution, where the strong interactions among segments as occurring in a melt system is absent, the line shape or the relaxation time distribution of the relaxation process $\langle P_2[\mathbf{u}(0)\cdot\mathbf{u}(t)]\rangle^2$ probed by the depolarized photon-correlation spectroscopy can actually be quite fully accounted for by including the effect of chain connectivity, regardless of the crudeness of the Rouse segment.

In the analysis leading to Eq. (28), the polymer molecule is modeled as a chain of freely jointed Kuhn segments. And it was shown that each Kuhn segment can be regarded as a correlated domain along the polymer (polystyrene) chain, whose collective motion is probed by the depolarized photon-correlation spectroscopy. As shown in the simulation that the difference between $\langle|\mathbf{b}|\rangle$ and $\langle b^2\rangle^{0.5}$ is very small, the Rouse segment and Kuhn segment can be regarded as equivalent. The results shown in Fig. 8 strongly support that the motion of a Rouse segment can actually be observed directly by the depolarized photon-correlation spectroscopy in the case of polystyrene. Furthermore, the estimated molecular weight for a Rouse segment $m=1100$ in the concentrated solutions obtained from analyzing the $\langle\tau_x\rangle/\tau_v$ ratio values is also of the same order of magnitude as the values $m=780-900$ obtained by other methods for the polystyrene melt. In a dilute polystyrene solution, m has been estimated to be as large as 5000 from the analysis of the oscillatory flow birefringence properties as a function of frequency.[26] It appears that the presence of solvent has some modification effect on the Rouse segment size. In our studied systems, the molecular weight dependence of viscosity indicates that the hydrodynamic interaction is basically entirely screened at least as far as the slow modes of motions are concerned. Whether the hydrodynamic interaction between beads one or two segments apart is also entirely screened can not be clearly judged based on the viscosity results alone. Some presence of hydrodynamic interaction at the local level is likely to have the effect to slow down slightly the highest mode of motion (i.e., the motion associated with a single Rouse segment).[3,28] This may contribute somewhat to our m value being slightly larger than those obtained for the polystyrene melt.

The motion $\langle P_2[\mathbf{u}(0)\cdot\mathbf{u}(t)]\rangle$ associated with a single Rouse segment in the melt observed by the depolarized photon-correlation spectroscopy cannot be well resolved due to its close overlapping with the sub-Rouse-segmental motions $f_s(t)$ in the time scale. The overlap of the $f_s(t)$ and $\langle P_2[\mathbf{u}(0)\cdot\mathbf{u}(t)]\rangle$ dynamic processes should be due to the strong energetic interactions among the chemical segments contacting each other closely in the melt state. In a concentrated solution, such energetic interactions are prevented from occurring by the mobile solvent molecules surrounding the segments. This allows us to compare the observed chain dynamics in the concentrated solutions with the Monte Carlo simulation results.

ACKNOWLEDGMENTS

This work is supported by the National Science Council (NSC 88-2113-M-009-004), and the simulation is carried out at the National Center for High-Performance Computing.

APPENDIX

When we compared the experimental results with the simulation as reported in this paper, it was found that a mistake had been made in the procedure of removing the q^2-dependent ''leakage'' mode from the measured depolarized photon-correlation function $f(t)=g^2(t)-1$ [$\phi(t)^2$ in Ref. 10 is replaced by $f(t)$ here]. A correction is due here. To simplify the explanation, an abbreviated form is assumed. Let $f(t)=(c_1(t)+c_2(t))^2$, where $c_1(t)$ represents the field correlation function of the true dynamic depolarized scattering [containing both the $f_s(t)$ and $\langle P_2[\mathbf{u}(0)\cdot\mathbf{u}(t)]\rangle$ processes in Eq. (28)], while $c_2(t)$ is that due to the leakage of the diffusive mode of the isotropic scattering arising from the concentration fluctuation. The relaxation time distributions of $c_1(t)$ and $c_2(t)$ have been obtained from the MSVD analysis (Figs. 6 and 10 of Ref. 10). To obtain the true de-

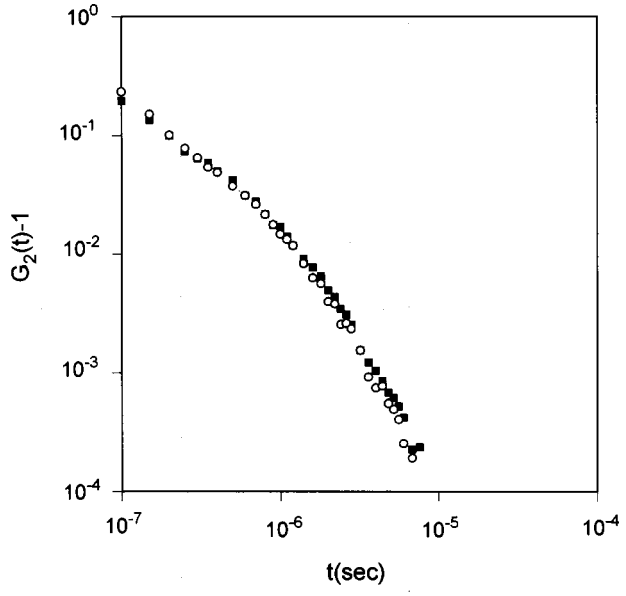

FIG. 9. The depolarized photon-correlation functions of S-F2 at $\theta=45°$ (■) and $\theta=90°$ (○) obtained by removing the q^2-dependent ''leakage'' mode from the measured correlation functions.

polarized photon-correlation function $c_1(t)^2$ from $f(t)$, the relation used should be $c_1(t)^2=[(f(t))^{0.5}-c_2(t)]^2$. What was shown in Figs. 7, 8, and 9 of Ref. 10 was obtained from $c_1(t)^2=f(t)-c_2(t)^2$. In other words, what were shown there contained an additional cross term $2c_1(t)c_2(t)$. Because the relaxation of $c_1(t)$ is much faster than that of $c_2(t)$, the cross term is dominated by the characteristics of $c_1(t)$. As a result, the q-dependence of $c_2(t)$ was basically not visible in the wrong correlation functions shown in Figs. 7, 8, and 9 of Ref. 10. The correct correlation functions showing the q-independence of $c_1(t)^2$ to replace those shown in Fig. 9 of Ref. 10 are shown in Fig. 9. The correction can be similarly applied to the other two figures. As these figures are basically for displaying the results of the MSVD analysis, which remain unchanged, the discussion and conclusion as presented in Ref. 10 are not effected by this mistake.

[1] P. E. Rouse, Jr., J. Chem. Phys. **21**, 1271 (1953).
[2] M. Doi and S. F. Edwards, *The Theory of Polymer Dynamics* (Oxford University Press, New York, 1986).
[3] R. B. Bird, C. F. Curtiss, R. C. Armstrong, and O. Hassager, *Dynamics of Polymeric Liquids*, 2nd ed. (Wiley, New York, 1987), Vol. 2.
[4] D. G. H. Ballard, M. G. Rayner, and J. Schelten, Polymer **17**, 349 (1976).
[5] T. Norisuye and H. Fujita, Polymer **14**, 143 (1982).
[6] T. Inoue, H. Okamoto, and K. Osaki, Macromolecules **24**, 5670 (1991).
[7] T. Inoue and K. Osaki, Macromolecules **29**, 1595 (1996).
[8] Y.-H. Lin, J. Polym. Res. **1**, 51 (1994).
[9] Y.-H. Lin and C. S. Lai, Macromolecules **29**, 5200 (1996).
[10] C. S. Lai, J.-H. Juang, and Y.-H. Lin, J. Chem. Phys. **110**, 9310 (1999).
[11] Y.-H. Lin, J.-H. Juang, and Z.-H. Luo (unpublished results).
[12] Y.-H. Lin, Macromolecules **17**, 2846 (1984); **19**, 159 (1986); **19**, 168 (1987); **20**, 885 (1987).
[13] Y.-H. Lin and J.-H. Juang, Macromolecules **32**, 181 (1999).
[14] D. J. Ferry, *Viscoelastic Properties of Polymers*, 3rd ed. (Wiley, New York, 1980).
[15] G. D. Patterson, C. P. Lindsey, and J. R. Stevens, J. Chem. Phys. **70**, 643 (1979).
[16] W. Brown and T. Nicolai, Macromolecules **27**, 2470 (1994).
[17] M. Fixman, J. Chem. Phys. **69**, 1538 (1978).
[18] D. L. Ermak and J. A. McCammon, J. Chem. Phys. **69**, 1352 (1978).
[19] M. P. Allen and D. J. Tildesley, *Computer Simulation of Liquids* (Oxford University Press, Oxford, 1989).
[20] J. W. Hennel and J. Klinowski, *Fundamentals of Nuclear Magnetic Resonance* (Longman Scientific & Technical, Essex, England, 1993).
[21] E. W. Fischer and M. Dettenmaier, J. Non-Cryst. Solids **31**, 181 (1978).
[22] E. G. Ehrenburg, E. P. Piskareva, and I. Y. A. Poddubnyi, J. Polym. Sci. C **42**, 1021 (1973).
[23] G. R. Alms, D. R. Bauer, J. I. Brauman, and R. Pecora, J. Chem. Phys. **59**, 5310 (1973).
[24] B. J. Berne and R. Pecora, *Dynamic Light Scattering* (Wiley, New York, 1976).
[25] M. Muthkumar and K. F. Freed, Macromolecules **10**, 899 (1977); **11**, 843 (1978).
[26] C. J. T. Martel, T. P. Lodge, M. G. Dibbs, T. M. Stokich, R. L. Sammler, C. J. Carriere, and J. L. Schrag, Faraday Symp. Chem. Soc. **18**, 173 (1983).
[27] B. Chu, *Laser Light Scattering* (Academic, San Diego, 1991).
[28] R. L. Sammler, J. L. Schrag, and A. S. Lodge, Exact Eigenvalue Spectra for Calculation of Dynamic Functions for Dilute Polymer Solutions Based on the Bead–Spring Model, University of Wisconsin Rheology Center Report No. 82, June 1982.